International Journal of Engineering & Technology, 7 (4.26) (2018) 146-152

International Journal of Engineering & Technology

Website: www.sciencepubco.com/index.php/IJET

Research paper



Blood Flow Modeling to Improve Cardiovascular Diagnostics: Application of A GTF to Predict Central Aortic Pressure using a 1-D Model

A. T. Butt[1], Y. A. Abakr[2]*, K. B. Mustapha[3]

[1]*Department of Mechanical, Materials and Manufacturing Engineering, University of Nottingham Malaysia Campus,*
[2]*Jalan Broga, Semenyih,43500, Selangor DE, Malaysia*
**Corresponding author E-mail: yousif.abakr@nottingham.edu.my*

Abstract

This study aims to demonstrate that a comprehensive one-dimensional model of the arterial network can be used in conjunction with the generalized transfer function (GTF) technique to estimate central aortic pressure using pressure waveforms obtained from peripheral sites. The peripheral and central pressure waveforms for a healthy subject are used to estimate transfer functions, which are then used to reconstruct central aortic pressure waveforms for a second model that simulates arterial stiffening. The similarities between the simulated aortic waveform and the waveforms estimated using the transfer function are 99.04%, 99.78% and 98.78% from the brachial, carotid and iliac arteries, respectively. The root-mean-square errors (RMSE) for the reconstructed waveforms from the brachial, carotid and iliac arteries are 2.36, 1.19 and 2.68 mmHg, respectively. The results from this study illustrate that the proposed method provides a feasible alternative to higher dimensional models as well as experimental studies and can greatly enhance the accuracy of central aortic pressure estimation.

Keywords: *Arterial network; Central aortic pressure; Computational fluid dynamics; One-dimensional modelling; Transfer function*

1. Introduction

In clinical diagnoses, a very important physiological index is blood pressure. There has been an increased interest in measuring the relationship between the central aortic pressure (the blood pressure at the aortic root) and peripheral pressure (for instance brachial, radial, carotid, femoral arteries) due to systolic hypertension being recognized as a risk factor for cardiovascular diseases [1]–[5]. The central aortic pressure represents the systemic after load on the heart. However, measuring the central aortic pressure in routine clinical practice is tedious, expensive and invasive, therefore pressures measured non-invasively such as sphygmomanometer, carotid artery tonometry [6]–[8] and brachial oscillometry [9]–[12] in peripheral locations are used as estimates of the central aortic pressure.

Previous research has shown that the waveforms of peripherally measured pressure and central aortic pressures are significantly different in regards to the wave shapes as well as amplitude [13]. It has been shown that the peripheral systolic pressure when compared to central aortic pressure is 11-22 mmHg higher [2]. It has also been shown that a number of blood pressure-lowering drugs have similar effects on the peripheral pressure but very different effects on the central aortic pressure [14], implying that central aortic pressure is a better indicator physiologically for diagnosing diseases [15]–[17].

In view of these findings, a statistics-based technique called the generalized transfer function (GTF) technique was proposed [2], [18]. This technique allows estimation of central aortic pressure from peripheral pressure measured non-invasively. Multiple central and peripheral pressures undergo a Fourier analysis and a generalized transfer function is calculated. The central pressures of individual patients can be estimated by simply multiplying this GTF to peripheral pressures of these patients in the frequency domain and converting the result back to the time domain [19]–[24]. The patent to this technique [25] is in use of SphygmoCor® system (SphygmoCor®,AtCor Medical, West Ryde, NSW, Australia), a commercially available blood pressure measurement equipment. However, there has been some debate that the general transfer function varies from person-to-person due to a variety of physiological differences, making the general transfer function an unreliable tool of choice in such analysis as it lacks adaptability [26] [27], [28]. Cloud et al. [27] undertook a study with 30 patients and found that the SphygmoCor® system underestimated the systolic central aortic pressure and overestimated the diastolic central aortic pressure by 13.3mmHg and 11.5mmHg, respectively. To put things into perspective, a blood pressure measuring equipment should not have a standard deviation greater than ±8mmHg [29]. Consequently, individualized transfer functions (ITF) were introduced to account for individual differences amongst patients [30]–[33], and although promising, they still lack complete personalization.

Pressure changes in arteries can be more accurately analyzed by deriving and solving the mathematical equations that govern the pressure wave dynamics in the arteries [34]. This can serve as the judging tool to check the validity of the transfer function method. Research has already been carried out using numerical modelling of the pulse wave propagation to study the changes in flow as it goes from the heart towards the peripheral arteries. Stergiopulos et al.[35] used peripheral pressure and velocity to model the pulse wave transmission effect in a vessel segment. Based on the reflec-

Copyright © 2018 Authors. This is an open access article distributed under the Creative Commons Attribution License, which permits unrestricted use, distribution, and reproduction in any medium, provided the original work is properly cited.

tion coefficient in the periphery and the time taken for pulse wave transmission, a transfer function was defined that relates the central and peripheral pressures. Since the simulation is carried out on a vessel segment, it does not provide information about pressure in other parts of the arterial network. Segers et al. [36] and Thore et al. [37] used transmission line models to simulate pulse wave dynamics. These are simplified models that do not take into consideration non-linearities such as inhomogeneous vessel wall elasticity, vessel tapering etc. To date, a full-scale cardiovascular model has not been used to systematically evaluate the GTF technique.

The aim of this paper is to demonstrate that a comprehensive cardiovascular model, specifically a one-dimensional model of the arterial network can be used together with the GTF technique to estimate central aortic pressure from peripheral pressure waveforms. One-dimensional models have been successfully used for various applications in the past few decades [38]–[47] and were covered in the preliminary analyses paper. A one-dimensional model offers an independent means to assess the GTF technique while also being an alternative to experimental studies.

2. Methods

2.1. One-Dimensional Model

The one-dimensional model used in this paper is the one developed by Olufsen [48]. The propagation of blood in the systemic arteries is described by the incompressible axisymmetric Navier-Stokes equations. The equations are integrated over the cross-sectional area of an arterial segment to produce the one-dimensional model. The blood flow is modelled in a bifurcating binary tree of 29 vessels where each vessel is modelled as an impermeable axisymmetric compliant cylinder and the blood is assumed as an incompressible, homogeneous and Newtonian fluid with density, ρ and viscosity, μ. The geometry of the arterial tree is based on the paper by Olufsen [39] and imitates the geometry of physiological arteries (Table 1). This model permits all the important aspects of physiological fluid-structure interaction to be captured accurately without increasing the computational load. Additionally, more vessels can be easily simulated but the arterial tree has been simplified for this study as the aim is to study the application of one-dimensional modelling rather than the blood flow itself.

The model is divided into two parts; the large arteries and the small arteries. The large arteries originate at the heart and are truncated after a maximum of two generations. The small arteries and arterioles are joined at the distal ends of the large arteries and modelled as binary asymmetric structured trees. The small arteries do not imitate physiologically accurate data instead are based on statistical relationships estimated from literature [39].

Each arterial segment is assumed to taper exponentially and the radius, $r(x)$ is modelled via the following equation

$$r(x) = r_{in}\, e^{\log\left(\frac{r_{out}}{r_{in}}\right)\left(\frac{x}{L}\right)} = r_{in}\left(\frac{r_{out}}{r_{in}}\right)^{\frac{x}{L}} \tag{1}$$

Where, x is the position along the vessel, r_{in} is the inlet (or proximal) radius, r_{out} is the outlet (or distal) radius of the vessel and L is the length of the vessel [39].

It is assumed that the velocity profile of blood is parabolic across the cross-sectional area of the vessel, therefore a relationship between the cross-sectional area of the vessel, $A(x,t)$ and pressure, $p(x,t)$ exerted on the arterial wall can be defined as the following:

$$p(x,t) - p_0 = \frac{4}{3}\left(k_1 e^{k_2 r_0(x)} + k_3\right)\left(1 - \sqrt{\frac{A_0(x)}{A(x,t)}}\right) \tag{2}$$

Where p_0 is the diastolic (nominal) pressure, $r_0$is the equilibrium radius (the radius when the pressure is nominal) and $k_1, k_2\ and\ k_3$ define the elasticity of the vessel walls and are the same for all vessels.

2.1.1. Large Arteries

The continuity and momentum equations that govern the one-dimensional flow in large arteries are

$$\frac{\partial A}{\partial t} + \frac{\partial q}{\partial x} = 0 \tag{3}$$

$$\frac{\partial q}{\partial t} + \frac{\partial}{\partial x}\left(\frac{q^2}{A}\right) + \frac{A}{\rho}\frac{\partial p}{\partial x} = -\frac{2\pi v\, r}{\delta}\frac{q}{A} \tag{4}$$

Where, v is the kinematic viscosity $\left(\frac{\mu}{\rho}\right)$ and δ is the thickness of the boundary layer. Equations (1)-(4) are used to calculate the pressure $p(x,t)$ and flow $q(x,t)$ in each arterial segment. The detailed derivations of these equations can be found in [39].

Table 1: Geometrical data for the one-dimensional model. Parameters L, r_{in} and r_{out} are the length, inlet radius and outlet radius of the artery. r_{min} is the truncation radius of the structured trees while R and L denote right and left. r_{min} is defined for only terminal arteries.

Artery	$L\ (cm)$	$r_{in}\ (cm)$	$r_{out}\ (cm)$	$r_{min}\ (cm)$
Ascending aorta	7.0	1.25	1.14	-
Anonyma	3.5	0.7	0.7	-
L, R Subclavian and Brachial	43.0	0.44	0.28	0.01
Right common carotid	17.0	0.29	0.28	0.02
Aortic arch I	1.8	1.14	1.11	-
Left common carotid	19.0	0.29	0.28	0.03
Aortic arch II	1.0	1.11	1.09	-
Thoracic aorta	18.8	1.09	0.85	-
Celiac axis	3.0	0.33	0.30	0.02
Abdominal aorta I	2.0	0.85	0.83	-
Superior Mesenteric	5.0	0.33	0.33	0.02
Abdominal aorta II	2.0	0.83	0.80	-
L, R Renal	3.0	0.28	0.25	0.02
Abdominal aorta III	1.0	0.80	0.79	-
Inferior Mesenteric	4.0	0.20	0.18	0.01
Abdominal aorta IV	6.0	0.79	0.73	-
L, R External Iliac	6.5	0.45	0.43	-
Abdominal aorta V	3.0	0.73	0.70	-
L, R Femoral I	13.0	0.43	0.40	-
L, R Internal Iliac	4.5	0.20	0.20	0.01
L, R Deep femoral	11.0	0.20	0.20	0.01
L, R Femoral II	44.0	0.40	0.30	0.01

2.1.2. Boundary Conditions

In order to extend the above equations to an entire arterial network, three boundary conditions are imposed. Firstly, to the inlet of the arterial tree (inflow condition), secondly, at each vessel bifurcation in which a parent vessel bifurcates into two daughter vessels and lastly a boundary condition is imposed at the terminal ends of the tree (outflow condition).

For the inflow condition, an ejection profile acquired through clinical measurement of flow in the ascending aorta [39] is imposed. The ejection profile as a function of time is shown in Fig. 1. At bifurcations, it is assumed that there is no leakage, therefore, the flow going out of the parent vessel (P) must be equal to the sum of the flow going into the two daughter vessels (d_1, d_2)

$$q_P(\mathrm{L},\mathrm{t}) = q_{d_1}(0,\mathrm{t}) + q_{d_2}(0,t) \tag{5}$$

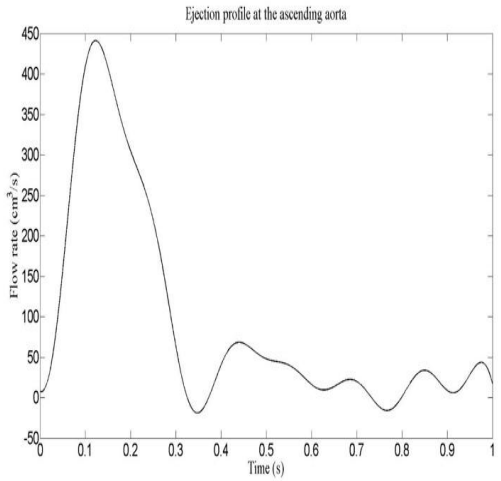

Fig. 1: Ejection profile used as the inflow boundary condition for the one-dimensional model.

At the bifurcation points, albeit minor, some energy is lost. This loss of energy can be accounted for by modelling it in terms of loss coefficients, however, these coefficients cannot be estimated analytically in a one-dimensional model [39]. A viable approximation of this energy loss is assuming continuity of pressure [4] at the bifurcation.

$$p_P(\mathrm{L},\mathrm{t}) = p_{d_1}(0,\mathrm{t}) = p_{d_2}(0,\mathrm{t}) \tag{6}$$

For the outflow condition, small arteries are joined to the terminal ends of the large arteries. These small arteries and arterioles are modelled as a structured tree and a semi analytical approach is used to express the root impedance of this tree. This in turn provides the outflow condition for the large arteries [48].

2.1.3. Small arteries

The small arteries and arterioles attached to the ends of the large arteries are modelled separately as binary asymmetric structured trees. Each of these small arteries keep bifurcating into generations of even smaller arteries until a specified radius, r_{min} has been reached (Table 1). The radii of the daughter vessels, r_{d_1} *and* r_{d_2} are linearly scaled, relative to the radius of the parent vessel, r_P via constants that characterize the asymmetry of the tree, α *and* β

$r_{d_1} = \alpha r_P$

$r_{d_2} = \beta r_P$

The values of α *and* β are taken as 0.9 and 0.6, respectively. The length of each vessel is determined using a length to radius ratio, $l_{rr} = \frac{L}{r_0} \approx 50$. These values are a calculated result of specific parameters that are beyond the scope of this paper but can be found in these papers [39], [49]–[52].

Similar to large arteries, the equations that govern blood propagation in small arteries can be derived from the axisymmetric form of Navier-Stokes equations. However viscous effects are more prominent in small arteries as compared to inertial effects hence the Navier-stokes equations can be linearized by neglecting the non-linear terms [39]. Once the equations are derived, they predict the flow $Q(x,\omega)$ and pressure $P(x,\omega)$ in the frequency domain. A no-slip boundary condition is used to link the equations together.

The continuity and momentum equations that govern the one-dimensional flow in small arteries are

$$\frac{i\omega}{CP} + \frac{\partial Q}{\partial x} = 0 \tag{7}$$

$$i\omega Q + K\frac{A_0}{\rho}\frac{\partial P}{\partial x} = 0 \tag{8}$$

where,

$$K = \begin{cases} 1 - \dfrac{2}{\sqrt{iw}} & for\ w > 4 \\ \dfrac{1}{\frac{4}{3} - \frac{8i}{w^2}} & for\ w \le 4 \end{cases}$$

and w is the Womersley parameter [53], [54] and $C = \frac{3A_0 r_0}{2Eh}$ is the compliance of the vessel in question [39] and ω is the angular frequency.

Combining equations (7) and (8) yields the wave equation as

$$\omega^2 \frac{\rho C}{KA_0} Q + \frac{\partial^2 Q}{\partial x^2} = 0 \tag{9}$$

Using the solution of equation (9) with equations (7) and (8) yields the equation for impedance (analogous to $R = \frac{V}{I}$ in electrical circuits)

$$Z = \frac{P}{Q} = -\frac{bcos(\omega x/c) - asin(\omega x/c)}{ig[acos(\omega x/c) + bsin(\omega x/c)]} \tag{10}$$

where, $g = \sqrt{\frac{CA_0K}{\rho}}$ and $c = \sqrt{\frac{A_{0K}}{\rho C}}$ while $a\ and\ b$ are constants of integration.

Inserting the expression for $\frac{b}{a}$ into equation (10) calculated at $x = 0$ the input impedance becomes

$$Z(0,\omega) = \frac{ig^{-1}\sin(\omega L/c) + Z(L,\omega)\cos(\omega L/c)}{\cos(\omega L/c) + igZ(L,\omega)\sin(\omega L/c)} \tag{11}$$

This can be extended to the entire tree by applying the boundary conditions at the small artery bifurcations similar to equations (5) and (6) yields

$$\frac{1}{Z_P} = \frac{1}{Z_{d_1}} + \frac{1}{Z_{d_2}} \tag{12}$$

Knowledge of g and L and the impedances at the terminals of the distance end allows using Equation (11) and (12) to compute the input impedance. Zero impedance is assumed at the distal terminals of the smaller arteries' tree. For an in depth derivation of the equations discussed above, see [39].

Using the equations described above, a one-dimensional model was set up to simulate a healthy human subject (Fig.2), using the parameters detailed in Table 2. The values of these parameters have been taken from the paper by Olufsen [39].

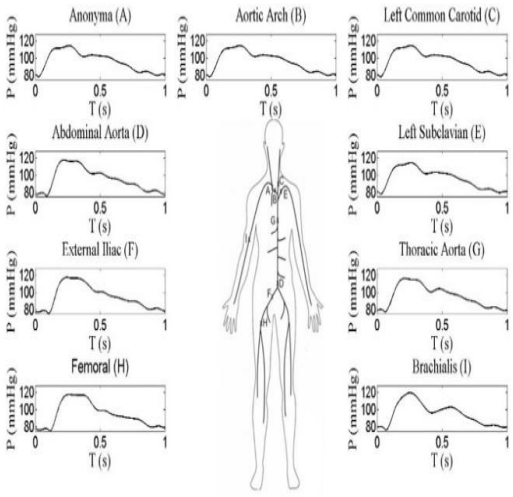

Fig2: Simulated pressures in various arterial segments

Table 2: Values of the model parameters.

Parameter	Unit	Value used
ρ	$g\ cm^{-3}$	1.055
μ	$g\ cm^{-1}\ s^{-1}$	0.049
p_0	$mmHg$	80
k_1	$g\ s^{-2}\ cm^{-1}$	2.0×10^7
k_2	cm^{-1}	-22.53
k_1	$g\ s^{-2}\ cm^{-1}$	8.65×10^5
α	-	0.9
β	-	0.6

2.2. Transfer Function

Each pressure wave comprises of harmonic waves at multiples of the frequency of the heart rate [23]. The generalized transfer function recreates the central aortic waveform from peripherally measured pressure waveform. Essentially, it is a ratio of the amplitudes and phase of the peripheral pressure waveform and the central pressure waveform [23]. A generalized transfer function of pressure waveforms between two sites is defined [2] as

$$H_{(A-B)} = \frac{P_B(\omega)}{P_A(\omega)} \tag{13}$$

where, $P_A(\omega)\ and\ P_B(\omega)$ are the pressure waveforms represented in the frequency domain at sites A and B, respectively and ω is the angular frequency. If the moduli are denoted as $M_A(\omega)\ and\ M_B(\omega)$ and phases denoted as $\varphi_A(\omega)\ and\ \varphi_B(\omega)$, the pressure waveforms can be written as $P_A(\omega) = M_A(\omega)e^{i\varphi}\ and\ P_B(\omega) = M_B(\omega)e^{i\varphi}$ for sites A and B, respectively.

For this study, site A is the ascending aorta while site B varies. It can be either the brachial artery, the common carotid artery or the iliac artery as will be seen in the next section.

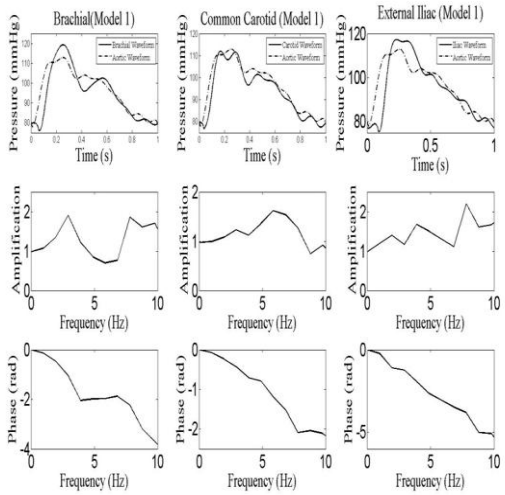

Fig3: Pressure waveform comparison and estimated transfer functions between the ascending aorta and brachial, carotid and iliac arteries.

2.3. Reconstruction of the Central Aortic Pressure

Once the model for a healthy human patient is simulated (Fig. 2), the pressure waveforms from site B (the brachial, common carotid and iliac arteries) are used in conjunction with the pressure waveform from site A (ascending aorta) to estimate a transfer function for each of the respective sites. This is done by first transforming the pressure waves into the frequency domain by using the discrete Fourier transform. Once the pressure waveforms have been transformed, equation (13) is applied to estimate the transfer function for each of these locations.

In order to simulate aging, the elasticity parameters of the model are changed to increase the stiffness of the vessels. This causes an increase in pressure and all the relevant changes in characteristics of the pressure waveforms that one would expect from aging (Fig. 4).

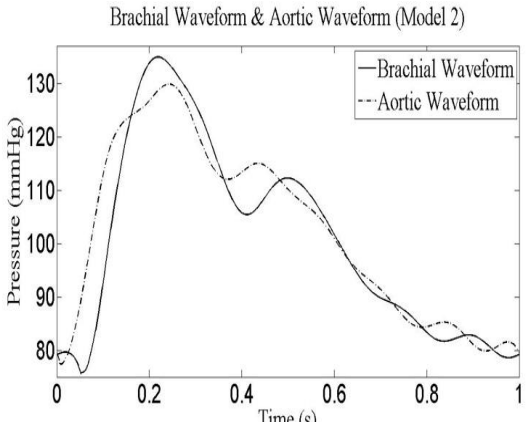

Fig4: Aortic and brachial pressure waveforms for the model that simulates arterial stiffening (Model 2).

The pressure waveforms of the brachial, carotid and Iliac arteries from the model simulating aging (Model 2) are transformed into the frequency domain again using DFT and then multiplied with their respective transfer functions (estimated using Model 1). The resulting complex values are transformed to the time domain using inverse DFT to reconstruct the aortic waveforms.

3. Results

It can be seen from the first simulated model (Model 1) that the systolic pressure increases towards the periphery while there is a slight decrease in the diastolic pressure. The brachial and ascending aortic pressure waves for Model 1 peak at 119.3mmHg and 112.9mmHg, respectively (Fig. 5). Downstream the dicrotic notch is also delayed and much smoother as compared to the dicrotic notch of the waveform near the aorta. The incoming pressure waves are also steeper near the periphery due to the variations in wave propagation. These variations are more prominent towards the periphery hence the steepness.

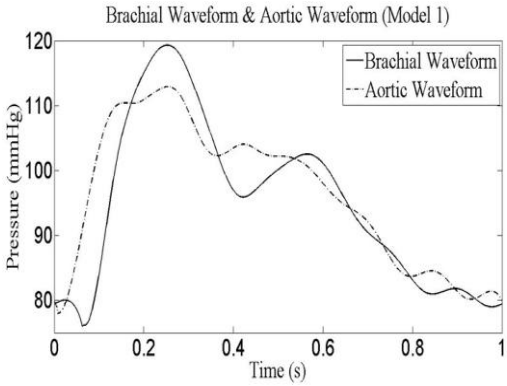

Fig5: Aortic and brachial pressure waveforms for the model that simulates a healthy subject (Model 1).

The pressure waveforms for Model 2 show that due to increased stiffness of the vessels, the systolic pressures of the aorta as well as the periphery are heightened. The brachial and ascending aortic pressure waves for Model 2 peak at 135mmHg and 129.8mmHg, respectively. The dicrotic notch is closer to the forward propagating wave because for the second model the elasticity parameters are readjusted to model arterial stiffening of the vessel walls (Fig. 4).

The modulus of the pressure transfer functions between the ascending aorta and the brachial artery, the carotid artery and the iliac artery all display characteristic peaking (Fig. 3).
The pressure transfer functions between the brachial artery, the carotid artery and iliac artery and the ascending aorta peak at 1.91, 1.62 and 2.196 at frequencies of 2.93Hz, 5.86Hz and 7.81Hz respectively. The phase' for all the arteries are negative as there is a delay between the frequency components of the pressure waves in the aorta and the respective arteries. All the phase' tend to reach an asymptotic values representing a constant group delay [2].
As mentioned before, the transfer functions estimated for all three arteries in Model 1 were used to reconstruct aortic waveforms in another model (Model 2). The aortic waveform for Model 2 was already simulated using the one-dimensional model and this known aortic waveform was compared with the aortic waveform reconstructed using the three transfer functions from Model 1.
Fig. 6A, 6B, 6C show the reconstructed aortic waveforms using the pressure waveforms from the brachial, common carotid and Iliac artery, respectively. The similarity between the actual aortic waveform and the waveform reconstructed using the generalized transfer function is 99.04%, 99.78% and 98.78% (2-D correlation coefficient, $r = 0.9904, 0.9978$ and 0.9878) from the respective peripheral locations.
The root-mean-square errors (RMSE) for the reconstructed waveforms from the brachial, common carotid and iliac arteries are 2.36, 1.19 and 2.68 mmHg, respectively. The systolic pressures estimated from the brachial, carotid and iliac arteries via the transfer functions are 4.78, 1.44 and 1.35 mmHg lesser than the actual aortic waveform.

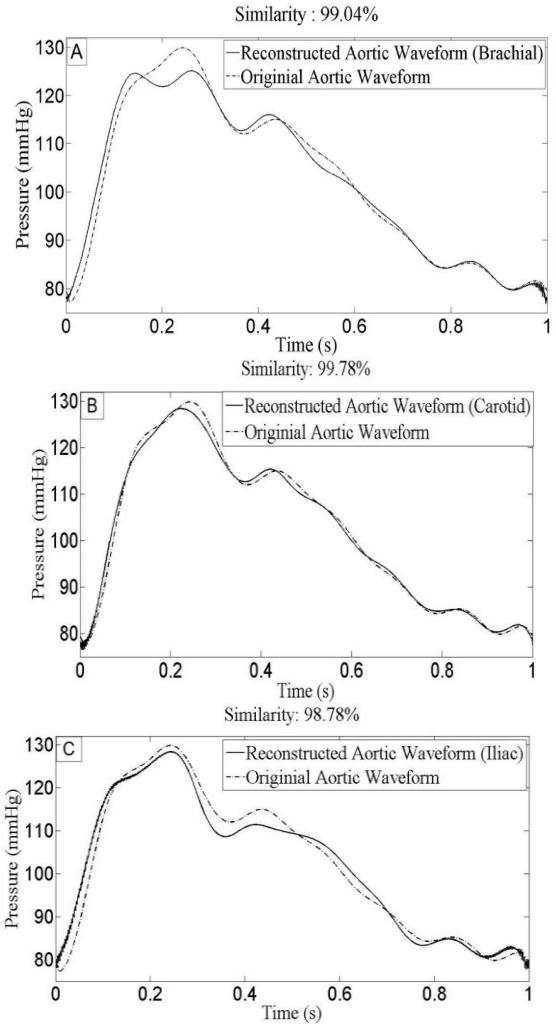

Fig. 6: Comparison of the aortic waveforms simulated using Model 2 and the aortic waveforms reconstructed using transfer functions for (A) Brachial artery, (B) Carotid artery and (C) Iliac artery.

4. Discussion

It has been previously shown that the waveforms in the ascending aorta and the waveforms in peripheral locations are markedly different [2], [13], [14]. The systolic pressure in the peripheral location is higher due to wave reflections that occur because of the tapering and bifurcating nature of the arteries and most importantly due to the impedances at the terminal ends of the arteries due to arterioles [55]. The reflected waves superimpose on the pressure waves, hence increasing the systolic pressure. The diastolic wave is also more prominent and due to the distance from the heart, the foot of the wave is delayed in peripheral locations. [56].
It has also been observed that aging leads to increased arterial stiffness as well as hypertension [57], [58] which in turn increase wave reflections. The reduced arterial distensibilty increases pulse wave velocity [13], [55], [59] which means the reflected waves from peripheral sites return earlier and superimpose on the systolic section of the pulse, increasing systolic pressure more than usual as well as making the diastolic wave less prominent. Additionally it has been observed that the difference between central and peripheral pulse is less obvious with aging [56].
For this study, two clinical scenarios were simulated. One for a young and healthy subject (Model 1) and the second for a slightly aged subject (Model 2). Aging was incorporated by increasing the stiffness of the vessels thus reducing the distensibilty of the vessels. Comparing the two models it is quite evident that for Model 2 (Fig. 4), both the systolic peaks are higher due to wave reflections and the diastolic wave is less prominent in the peripheral pulse as compared to the one in Model 1 (Fig. 5). The dicrotic notch for the peripheral pulse in Model 2 lasts for a lesser amount of time as compared to Model 1. Thus, showing that non-linearities and wave propagation effects were well captured by the model and the increased arterial stiffness, indeed, effected the waveforms as expected.
Transfer functions between the brachial, carotid and iliac arteries are estimated (Fig. 3) and used in model (2) to reconstruct the aortic waveform of Model 2 from each of these locations (Fig.6). The results discussed above show that the transfer function reconstructs the aortic waveform with good accuracy. However, the accuracy decreases the farther away the peripheral site is from the heart. The best estimation comes from the carotid artery because it is closest to the heart hence the waveform has not been modified as much as the other peripheral sites [60].
Limitations: Although the numerical model captures blood flow propagation with good precision and the similarities between the reconstructed and actual aortic waveforms demonstrate the capability of the transfer function, this is still a pilot study. It lacks experimental results to validate the effectiveness of the transfer function. In addition, the transfer function is known to lack adaptability to patient specific situations [26] [27], [28]. This study presents only one clinical scenario (arterial wall stiffening) which is a broad field of study and has various influences from multiple factors as opposed to just aging. In the near future, we plan to take this study a step further for the inclusion of modelling various diseased conditions in order to systematically assess the performance and validity of the transfer function.

5. Conclusion

Previous studies conducted to evaluate transfer functions have used transmission line or Windkessel/Windkessel-derived models, which do not take into consideration non-linearities of blood flow. Some models simulate isolated cases such as only the upper limbs. To our knowledge, little effort has been devoted to construct a comprehensive cardiovascular model that considers non-linearities as well as geometrical properties in conjunction with the transfer function technique. This study is based on a one-dimensional blood flow model proposed by Olufsen et al [39], [48]. This model is comprehensive and successfully incorporates non-linearities

such as vessel tapering, vessel branching as well as changes in vessel wall elasticity. This model is used in conjunction with the transfer function technique to estimate the central aortic pressure. Once this model is validated against experimental data and the validity of the transfer function is assessed, this model has the capability to provide an alternative to experimental studies in order to enhance the accuracy of central aortic pressure estimation.

Acknowledgement

This study was funded by MOSTI under grant number: 06-02-12-SF0247. The authors would like to thank Dr. Yubing Shi, University of Northampton. The authors would also like to extend their gratitude to the University of Nottingham, Malaysia Campus for their support and facilities.

References

[1] G. P. Gravlee, A. B. Wong, T. G. Adkins, L. Douglas Case, and A. L. Pauca, "A comparison of radial, brachial, and aortic pressures after cardiopulmonary bypass," *J. Cardiothorac. Anesth.*, vol. 3, no. 1, pp. 20–26, Feb. 1989.

[2] M. Karamanoglu, M. F. O'Rourke, a P. Avolio, and R. P. Kelly, "An analysis of the relationship between central aortic and peripheral upper limb pressure waves in man.," *Eur. Heart J.*, vol. 14, no. 2, pp. 160–167, 1993.

[3] R. P. Kelly, H. H. Gibbs, M. F. O'Rourke, J. E. Daley, K. Mang, J. J. Morgen, and A. P. Avolio, "Nitroglycerin has more favourable effects on left ventricular afterload than apparent from measurement of pressure in a peripheral artery," *Eur. Heart J.*, vol. 11, no. 2, pp. 138–144, 1990.

[4] N. Stergiopulos, D. F. Young, and T. R. Rogge, "Computer simulation of arterial flow with applications to arterial and aortic stenoses," *J. Biomech.*, vol. 25, no. 12, pp. 1477–1488, 1992.

[5] M. Karamanoglu, D. E Gallagher, A. Avolio, and M. F O'Rourke, "Pressure wave propagation in a multibranched model of the human upper limb," *Am. J. Physiol.*, vol. 269, pp. H1363-9, 1995.

[6] G. M. Drzewiecki, J. Melbin, and A. Noordergraaf, "Arterial tonometry: Review and analysis," *J. Biomech.*, vol. 16, no. 2, pp. 141–152, 1983.

[7] R. P. Kelly, M. Karamanoglu, H. Gibbs, A. P. Avolio, and M. F. O'Rourke, "Noninvasive carotid pressure wave registration as an indicator of ascending aortic pressure," *J. Vasc. Med. Biol.*, vol. 1, pp. 241–247, 1989.

[8] R. P. Kelly, C. Hayward, J. Ganis, J. Daley, A. P. Avolio, and M. F. O"Rourke, "Noninvasive registration of the arterial pressure pulse waveform; using high-fidelity applanation tonometry," *J. Vasc. Med. Biol.*, vol. 1, pp. 142–149, 1989.

[9] W. J. Verberk, H. Cheng, L.-C. Huang, C.-M. Lin, Y.-P. Teng, and C.-H. Chen, "Practical Suitability of a Stand-Alone Oscillometric Central Blood Pressure Monitor: A Review of the Microlife WatchBP Office Central," *Pulse*, vol. 3, no. 3–4, pp. 205–216, 2016.

[10] J. E. Lewis, P. Williams, and J. H. Davies, "Non-invasive assessment of peripheral arterial disease: Automated ankle brachial index measurement and pulse volume analysis compared to duplex scan," *SAGE Open Med.*, vol. 4, no. 5, p. 205031211665908, 2016.

[11] Y. Watanabe, H. Masaki, Y. Yunoki, A. Tabuchi, I. Morita, S. Mohri, and K. Tanemoto, "Ankle-Brachial Index, Toe-Brachial Index, and Pulse Volume Recording in Healthy Young Adults," *Ann. Vasc. Dis.*, vol. 8, no. 3, pp. 227–235, 2015.

[12] R. E. D. Climie, M. G. Schultz, S. B. Nikolic, K. D. K. Ahuja, J. W. Fell, and J. E. Sharman, "Validity and reliability of central blood pressure estimated by upper arm oscillometric cuff pressure," *Am. J. Hypertens.*, vol. 25, no. 4, pp. 414–420, 2012.

[13] W. Nichols, M. O'Rourke, and C. Vlachopoulos, "Mcdonald's Blood Flow in Arteries," *Shock*, vol. 9, no. 6, p. 456, 1998.

[14] B. Williams, P. S. Lacy, S. M. Thom, K. Cruickshank, A. Stanton, D. Collier, A. D. Hughes, H. Thurston, and M. O'Rourke, "Differential impact of blood pressure-lowering drugs on central aortic pressure and clinical outcomes: Principal results of the Conduit Artery Function Evaluation (CAFE) study," *Circulation*, vol. 113, no. 9, pp. 1213–1225, 2006.

[15] M. E. Safar, J. Blacher, B. Pannier, A. P. Guerin, S. J. Marchais, P.-M. Guyonvarc\textquoterighth, and G. M. London, "Central Pulse Pressure and Mortality in End-Stage Renal Disease," *Hypertension*, vol. 39, no. 3, pp. 735–738, 2002.

[16] T. K. Waddell, A. M. Dart, T. L. Medley, J. D. Cameron, and B. A. Kingwell, "Carotid Pressure Is a Better Predictor of Coronary Artery Disease Severity Than Brachial Pressure," *Hypertension*, vol. 38, no. 4, pp. 927–931, 2001.

[17] M. J. Roman, R. B. Devereux, J. R. Kizer, E. T. Lee, J. M. Galloway, T. Ali, J. G. Umans, and B. V. Howard, "Central pressure more strongly relates to vascular disease and outcome than does brachial pressure: The strong heart study," *Hypertension*, vol. 50, no. 1, pp. 197–203, 2007.

[18] C.-H. Chen, E. Nevo, B. Fetics, P. H. Pak, F. C. P. Yin, W. L. Maughan, and D. A. Kass, "Estimation of Central Aortic Pressure Waveform by Mathematical Transformation of Radial Tonometry Pressure," *Circulation*, vol. 95, no. 7, pp. 1827–1836, 1997.

[19] B. Fetics, E. Nevo, C. H. Chen, and D. A. Kass, "Parametric model derivation of transfer function for noninvasive estimation of aortic pressure by radial tonometry," *IEEE Trans. Biomed. Eng.*, vol. 46, no. 6, pp. 698–706, 1999.

[20] A. L. Pauca, M. F. O'Rourke, and N. D. Kon, "Prospective evaluation of a method for estimating ascending aortic pressure from the radial artery pressure waveform.," *Hypertension*, vol. 38, no. 4, pp. 932–937, 2001.

[21] S. Soderstrom, G. Nyberg, M. F. O'Rourke, J. Sellgren, and J. Pontén, "Can a clinically useful aortic pressure wave be derived from a radial pressure wave?," *Br. J. Anaesth.*, vol. 88, no. 4, pp. 481–488, 2002.

[22] D. Gallagher, A. Adji, and M. O'Rourke, "Validation of the transfer function technique for generating central from peripheral upper limb pressure waveform," *Am. J. Hypertens.*, vol. 17, no. 11, pp. 1059–1067, 2004.

[23] J. E. Sharman, R. Lim, A. M. Qasem, J. S. Coombes, M. I. Burgess, J. Franco, P. Garrahy, I. B. Wilkinson, and T. H. Marwick, "Validation of a generalized transfer function to noninvasively derive central blood pressure during exercise," *Hypertension*, vol. 47, no. 6, pp. 1203–1208, 2006.

[24] T. Weber, S. Wassertheurer, M. Rammer, E. Maurer, B. Hametner, C. C. Mayer, J. Kropf, and B. Eber, "Validation of a brachial cuff-based method for estimating central systolic blood pressure," *Hypertension*, vol. 58, no. 5, pp. 825–832, 2011.

[25] M. F. O'Rourke, "Method for Ascertaining the Pressure Pulse and Related Parameters in the Ascending Aorta from the Contour of the Pressure Pulse in the Peripheral Arteries," US 5,265,011, 1993.

[26] W. J. Stok, "Changes in finger-aorta pressure transfer function during and after exercise," *J. Appl. Physiol.*, vol. 101, no. 4, pp. 1207–1214, 2006.

[27] G. C. Cloud, C. Rajkumar, J. Kooner, J. Cooke, and C. J. Bulpitt, "Estimation of central aortic pressure by SphygmoCor requires intra-arterial peripheral pressures.," *Clin. Sci. (Lond).*, vol. 105, no. 2, pp. 219–225, 2003.

[28] P. Segers, D. Mahieu, J. Kips, E. Rietzschel, M. De Buyzere, D. De Bacquer, S. Bekaert, G. De Backer, T. Gillebert, P. Verdonck, and L. Van Bortel, "Amplification of the pressure pulse in the upper limb in healthy, middle-aged men and women," *Hypertension*, vol. 54, no. 2, pp. 414–420, 2009.

[29] W. B. White, A. S. Berson, C. Robbins, M. J. Jamieson, L. M. Prisant, E. Roccella, and S. G. Sheps, "National standard for measurement of resting and ambulatory blood pressures with automated sphygmomanometers," *Hypertension*, vol. 21, no. 4, pp. 504–509, 1993.

[30] G. Swamy, Q. Ling, T. Li, and R. Mukkamala, "Blind identification of the aortic pressure waveform from multiple peripheral artery pressure waveforms.," *Am. J. Physiol. Heart Circ. Physiol.*, vol. 292, no. 5, pp. H2257-64, 2007.

[31] J. O. Hahn, A. T. Reisner, F. A. Jaffer, and H. H. Asada, "Subject-specific estimation of central aortic blood pressure using an individualized transfer function: A preliminary feasibility study," *IEEE Trans. Inf. Technol. Biomed.*, vol. 16, no. 2, pp. 212–220, 2012.

[32] G. Swamy, D. Xu, N. B. Olivier, and R. Mukkamala, "An adaptive transfer function for deriving the aortic pressure waveform from a peripheral artery pressure waveform," *Am. J. Physiol. Circ. Physiol.*, vol. 297, no. 5, pp. H1956–H1963, 2009.

[33] N. Fazeli, M. Rashedi, A. Chappell, S. Wang, R. Macarthur, M. S. Mcmurtry, B. Finegan, and J. Hahn, "Subject - Specific Estimation of Aortic Blood Pressure via System Identification : Preliminary In - Human Experimental Study *," 2013.

[34] Y. Shi, P. Lawford, and R. Hose, "Review of zero-D and 1-D models of blood flow in the cardiovascular system.," *Biomed. Eng.*

Online, vol. 10, no. 1, p. 33, 2011.
[35] N. Stergiopulos, B. E. Westerhof, and N. Westerhof, "Physical basis of pressure transfer from periphery to aorta: a model-based study," *Am. J. Physiol. Circ. Physiol.*, vol. 274, no. 4, pp. H1386–H1392, 1998.
[36] P. Segers, S. Carlier, a Pasquet, S. I. Rabben, L. R. Hellevik, E. Remme, T. De Backer, J. De Sutter, J. D. Thomas, and P. Verdonck, "Individualizing the aorto-radial pressure transfer function: feasibility of a model-based approach.," *Am. J. Physiol. Heart Circ. Physiol.*, vol. 279, no. 2, pp. H542-9, 2000.
[37] C.-J. Thore, J. Stålhand, and M. Karlsson, "Toward a noninvasive subject-specific estimation of abdominal aortic pressure.," *Am. J. Physiol. Heart Circ. Physiol.*, vol. 295, no. 3, pp. H1156–H1164, 2008.
[38] M. S. Olufsen, "Structured tree outflow condition for blood flow in larger systemic arteries.," *Am J Physiol*, vol. 276, no. 1 Pt 2, pp. H257--H268, 1999.
[39] M. S. Olufsen, C. S. Peskin, W. Y. Kim, E. M. Pedersen, A. Nadim, and J. Larsen, "Numerical simulation and experimental validation of blood flow in arteries with structured-tree outflow conditions," *Ann. Biomed. Eng.*, vol. 28, no. 11, pp. 1281–1299, 2000.
[40] K. S. Matthys, J. Alastruey, J. Peiró, A. W. Khir, P. Segers, P. R. Verdonck, K. H. Parker, and S. J. Sherwin, "Pulse wave propagation in a model human arterial network: assessment of 1-D numerical simulations against in vitro measurements.," *J. Biomech.*, vol. 40, no. 15, pp. 3476–3486, 2007.
[41] N. Stergiopulos, "Computer simulation of arterial blood flow," 1990.
[42] S. J. Sherwin, V. Franke, J. Peiró, and K. Parker, "One-dimensional modelling of a vascular network in space-time variables," *J. Eng. Math.*, vol. 47, no. 3–4, pp. 217–250, 2003.
[43] J. Lee and N. P. Smith, "Development and application of a one-dimensional blood flow model for microvascular networks.," *Proc. Inst. Mech. Eng. H.*, vol. 222, no. 4, pp. 487–511, 2008.
[44] P. Reymond, F. Merenda, F. Perren, D. Rüfenacht, and N. Stergiopulos, "Validation of a one-dimensional model of the systemic arterial tree.," *Am. J. Physiol. Heart Circ. Physiol.*, vol. 297, no. 1, pp. H208–H222, 2009.
[45] X. Wang, "1D modeling of blood ow in networks : numerical computing and applications.", Ph.D. dissertation, Universitie Pierre et Marie Curie - Paris VI, 2014.
[46] A. Noordergraaf, *Circulatory System Dynamics*. 1978.
[47] F. N. van de Vosse, "Mathematical modelling of the cardiovascular system," *J. Eng. Math.*, vol. 47, no. 3, pp. 175–183, 2003.
[48] M. S. Olufsen, "Structured tree outflow condition for blood flow in larger systemic arteries.," *Am J Physiol*, vol. 276, no. 1 Pt 2, pp. H257--H268, 1999.
[49] C. D. Murray, "The physiological principle of minimum work applied to the angle of branching of arteries," *J. Gen. Physiol.*, vol. 9, no. 6, pp. 835–841, 1926.
[50] M. S. Pollanen, "Dimensional optimization at different levels of the arterial hierarchy," *J. Theor. Biol.*, vol. 159, no. 2, pp. 267–270, 1992.
[51] H. B. M. Uylings, "Optimization of diameters and bifurcation angles in lung and vascular tree structures," *Bull. Math. Biol.*, vol. 39, no. 5, pp. 509–520, 1977.
[52] G. L. Papageorgiou, B. N. Jones, V. J. Redding, and N. Hudson, "The area ratio of normal arterial junctions and its implications in pulse wave reflections," *Cardiovasc. Res.*, vol. 24, no. 6, pp. 478–484, 1990.
[53] H. B. Atabek, "Wave Propagation through a Viscous Fluid Contained in a Tethered, Initially Stressed, Orthotropic Elastic Tube," *Biophys. J.*, vol. 8, no. 5, pp. 626–649, 1968.
[54] T. Pedley, *The Fluid Mechanics of Large Blood Vessels*. Cambridge,G.B.: Cambridge University Press, 1980.
[55] M. F. O'Rourke, *Arterial function in health and disease*. Newyork , USA: Churchill Livingstone, 1982.
[56] M. F. O'Rourke and T. Yaginuma, "Wave reflections and the arterial pulse.," *Arch. Intern. Med.*, vol. 144, no. 2, pp. 366–371, 1984.
[57] I. Ferreira, R. J. van de Laar, M. H. Prins, J. W. Twisk, and C. D. Stehouwer, "Carotid Stiffness in Young Adults: A Life-Course Analysis of its Early Determinants," *Hypertension*, vol. 59, no. 1, pp. 54–61, 2012.
[58] M. AlGhatrif, J. B. Strait, C. H. Morrell, M. Canepa, J. Wright, P. Elango, A. Scuteri, S. S. Najjar, L. Ferrucci, and E. G. Lakatta, "Longitudinal Trajectories of Arterial Stiffness and the Role of Blood PressureNovelty and Significance," *Hypertension*, vol. 62, no. 5, pp. 934–941, 2013.
[59] M. F. O'Rourke, "Vascular impedance in studies of arterial and cardiac function.," *Physiol. Rev.*, vol. 62, no. 2, pp. 570–623, 1982.
[60] S. C. Millasseau, S. J. Patel, S. R. Redwood, J. M. Ritter, and P. J. Chowienczyk, "Pressure wave reflection assessed from the peripheral pulse: Is a transfer function necessary?," *Hypertension*, vol. 41, no. 5, pp. 1016–1020, 2003.